J. Radiat. Res., 45, 373–384 (2004) *Review Article*

Recent Progress in *In Vivo* ESR Spectroscopy

Keizo TAKESHITA and Toshihiko OZAWA*

***In vivo* ESR/Free radicals/Redox/Partial oxygen pressure/Oxidative stress**

The generation of free radicals and redox status is related to various diseases and injuries that are related to radiation, aging, ischemia-reperfusion, and other oxidative factors. *In vivo* electron spin resonance (ESR) spectroscopy is noninvasive and detects durable free radicals in live animals. ESR spectrometers for *in vivo* measurements operate at a lower frequency (~3.5 GHz, ~1 GHz, 700 MHz, and ~300 MHz) than usual (9-10 GHz). Several types of resonators have been designed to minimize the dielectric loss of electromagnetic waves caused by water in animal bodies. *In vivo* ESR spectroscopy and its imaging have been used to analyze radical generation, redox status, partial pressure of oxygen and other conditions in various disease and injury models related to oxidative stress with probes, such as nitroxyl radicals. Through these applications, the clarification of the mechanisms related to oxidative diseases (injuries) and the accumulation of basic data for radiological cancer therapy are now ongoing. *In vivo* ESR measurement is performed in about 10 laboratories worldwide, including ours. To introduce *in vivo* ESR spectroscopy to life scientists, this article reviews the recent progress of *in vivo* ESR spectroscopy in instrumentation and its application to the life sciences.

INTRODUCTION

Ever since the suggestion of a relationship between reactive oxygen species and disease (or aging), the measurement of biological free radicals and redox states has been a popular research topic. Electron spin resonance (ESR) spectroscopy is the most reliable technique for this purpose because it measures only paramagnetic species having unpaired electrons, such as free radicals and transition metal complexes. This technique has been used *in vitro* to measure oxygen radicals such as hydroxyl radical ($^{\cdot}OH$) and superoxide anion radical ($O_2^{\cdot -}$) in combination with the spin-trapping technique[1]. The measurement of ESR is nondestructive and is unaffected by the turbidity of the sample, so people are interested in using ESR for the *in vivo* measurement of biological radicals. However, there are difficulties with this. First, steady concentrations of biological radicals are too low to detect directly with ESR spectroscopy during their very short half-life. Second, water in the body of the animal causes dielectric loss of the electromagnetic waves used for ESR measurement. In this article, an outline of *in vivo* ESR is given first, and recent applications of this technique are then summarized.

*Corresponding author: Phone: +81-43-206-3002,
Fax: +81-43-256-6282,
E-mail: ozawa@nirs.go.jp
Redox Regulation Research Group, National Institute of Radiological Sciences, 9-1, Anagawa-4, Inage-ku, Chiba 263-8555, Japan.

ESR SPECTROSCOPY AND DEVELOPMENT OF THE *IN VIVO* ESR SPECTROMETER

ESR spectroscopy, like nuclear magnetic resonance (NMR) spectroscopy, is a kind of magnetic resonance spectroscopy. The spin of an electron produces a magnetic moment. Electromagnetic wave radiation of the appropriate frequency under a given external magnetic field causes the excitation of unpaired electrons from the lower energy level to the higher level by the interaction of the magnetic moment of electron spin with the magnetic component of the electromagnetic wave (magnetic resonance). ESR spectroscopy is usually done by the use of continuous wave (CW) methods, in which a continuous radiation of electromagnetic waves is applied to the sample and magnetic resonance is detected by slowly sweeping the external magnetic field. The ESR spectrometer detects the absorption of the energy of the electromagnetic wave at the resonance frequency. The ESR of *in vitro* samples is conventionally measured with X-band electromagnetic wave (9-10 GHz). Because the dielectric loss of electromagnetic wave is high at this frequency, a small volume (less than 100 μL) of aqueous sample is taken in a thin quartz cell for the measurement. The penetration of the electromagnetic wave depends on the dielectric constant and conductivity of tissues and the frequency of the electromagnetic wave applied. Halpern and Bowman[2] plotted the penetration depth of electromagnetic wave in a cylindrical geometry as a function of electromagnetic wave frequency.

In this plot, the radius of the muscle equivalent cylinder (for which the magnitude of magnetic field of electromagnetic wave along the center axis has fallen to $1/e$ of its surface value) is only ~1 mm at X-band. However, the radius increases with a decrease in the frequency; approximately 16 mm at L-band (~1 GHz) and approximately 55 mm at 250 MHz. Thus the use of lower frequencies is essential for the *in vivo* application of ESR, especially whole-body measurement of small animals, at the expense of sensitivity. The first noninvasive study was reported in 1983 by Lukiewicz and Lukiewicz[3]. They injected durable nitroxyl radical to mouse, and ESR measurement was carried out at L-band in whole body or in melanoma implanted into the tail of the mouse. Subsequently, Berliner *et al.*[4] imaged the distribution of nitroxyl radical in the melanoma. After these reports, several research groups actively developed the *in vivo* ESR spectrometer and began the *in vivo* measurement with live animals. S-band (~3.5 GHz) has been used for the measurement of the tail[5–7]. L-band (~1 GHz) has been widely used to measure durable nitroxyl radical in the mouse head, chest, and abdomen[8–13]. For whole-body measurement of rats, lower frequencies (280-700 MHz) should be used[14–18]. The term radio frequency (RF) in this article indicates the region of electromagnetic wave used for *in vivo* ESR spectroscopy.

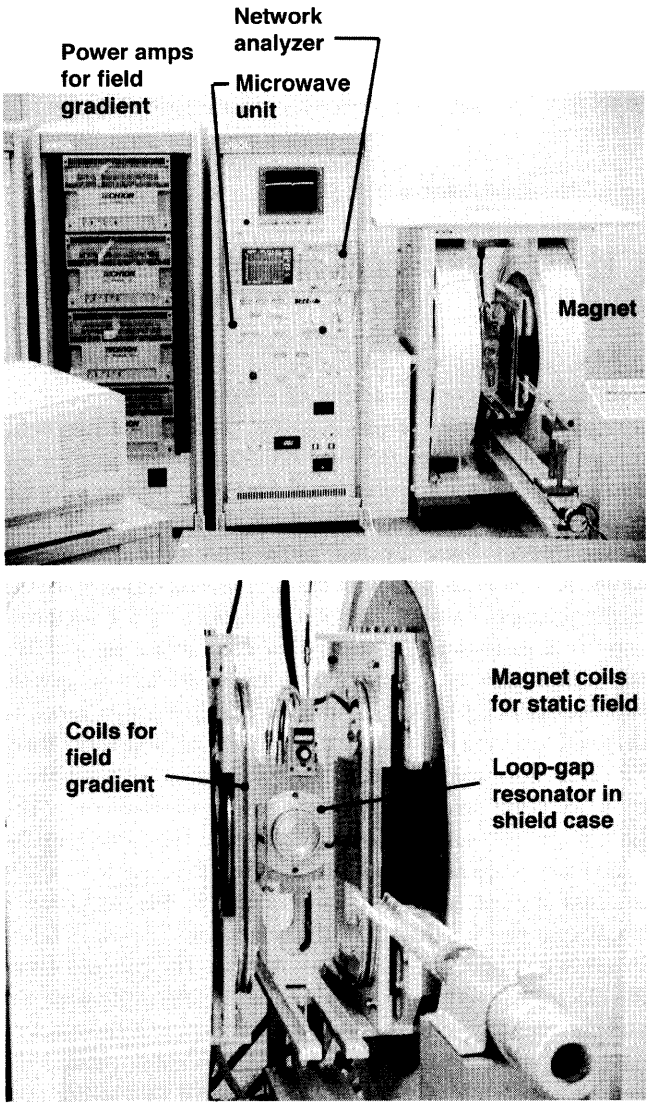

Fig. 1. ESR-CT system (JEOL, Ltd.)

The ESR spectrum recorded under a linear field gradient includes one-dimensional spatial information. To extract the spatial information, the spectrum is deconvoluted with a spectrum recorded under no gradient. The distribution of radicals can typically be imaged by the use of reconstruction methods such as back projection with the one-dimensional radical distributions obtained under field gradients in various directions (refer to reviews[19, 20]). First, a one-dimensional image at L-band was reported by Berliner and Fujii with a celery sample soaked in an aqueous solution of nitroxyl radical[21]. Figure 1 shows an ESR imaging system in our laboratory.

RESONATORS FOR *IN VIVO* ESR

Cylindrical and rectangular cavity resonators with specific wave guide modes are commonly used for the X-band ESR spectrometer. In these resonators, a small volume sample receives a high density RF magnetic component to obtain high sensitivity. To apply ESR to *in vivo* measurements, however, the geometrical shape and dimension of the resonator should be suitable for animal measurements. The resonators for *in vivo* ESR spectroscopy are classified into two types.

(i) Volume-coil-type resonators

An animal (or a part of an animal) is placed in the resonator, and radicals distributed in the body are measured. This resonator is suitable for whole body measurement of radicals and imaging of the distribution of the radicals.

(ii) Surface-coil-type resonators

The resonator is put on the surface of the animal body (or an organ) like a stethoscope, and radicals present near the resonator are measured rather selectively. This resonator is suitable for the topical measurement of radicals.

The sensitivity of ESR is proportional to the quality factor (Q) of the resonator and the filling factor (η), which is the RF magnetic field-squared weighted fraction of the resonator volume occupied by the sample[22].

The dielectric loss of electromagnetic waves is caused by interaction between the RF electric component and the aqueous sample. Thus the separation of the RF electric field from the RF magnetic field is important for an accurate ESR measurement. The following resonators were designed for this purpose.

Loop-gap resonator

This resonator is similar in design to magnetrons and heavy ion particle accelerators and was first used for ESR by

Froncisz and Hyde[23]. It consists of a loop divided into sections by one or more gaps (Fig. 2). An inductive coupler is used to match the RF line to the resonator by mechanically changing the separation of the coupling loop and the resonator loop. The loop and gap parts of this resonator operate as inductive coil and capacitors, respectively. The capacitive and inductive elements are separated in space, and the RF magnetic field inside the loop is fairly separated from the RF electric field around the gaps. The advantage of this design is that a resonator with a large diameter can be built by increasing the number of gaps. A large diameter resonator needs a shield case to block electromagnetic wave radiation.

The leakage of the RF electric component into the sample space sometimes reduces the Q value and shifts the resonance frequency when the resonator contains a sample with large dielectric constant. Ono *et al.*[24] shielded gaps on the inside of the resonator loop to prevent leakage of the RF electric component into the sample space (a bridged loop-gap resonator). This approach is valid for the measurement of a relatively large animal. Recently, Ono *et al.*[25] evaluated the relationship between magnetic field homogeneity in the sample space and the size of the electric shielding plate. The optimum bridge angle to obtain homogeneous sensitivity in the sample space of a loop-gap resonator (70 mm in diameter, 2 gaps) with a resonance frequency of 302 MHz was 80–100°. Zweier and Kuppusamy[26] separately reported that recessing the gaps of the resonator (1.1 GHz) with semicylindrical holes decreased the fringe of the RF electric field in the sample space, resulting in a decrease in dielectric loss.

A loop-gap resonator was also used as a surface-coil-type resonator using leakage of an RF magnetic component at one end of the loop, not only as a volume-coil-type resonator[27].

Re-entrant resonator

The re-entrant resonator was originally developed by Sotgiu *et al.*[28,29] and is typically composed of two circular channels surrounding central gaps (Fig. 3). An animal is inserted into the center arm, and an inductive coupler loop is inserted into one of the two lateral arms. Matching between the resonator and the RF line is performed by rotating the coupling loop. There is an RF electric field in the gap (re-entrant), and an RF magnetic field distributes in the

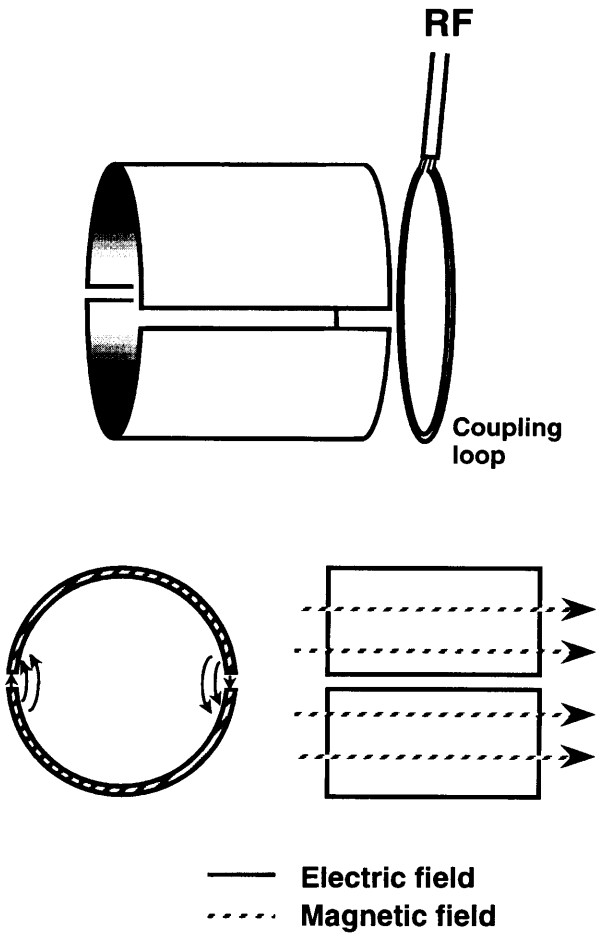

Fig. 2. Loop-gap resonator with two-gaps. Matching of the RF line to the resonator is performed by mechanically changing the distance between the coupling loop and the resonator loop.

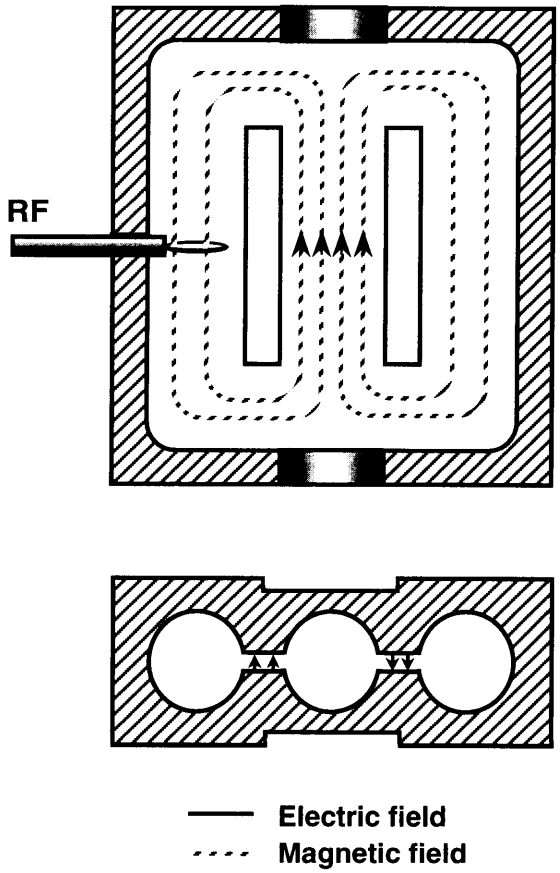

Fig. 3. Re-entrant resonator. Matching of the RF line to the resonator is performed by rotating the coupling loop.

channels to form a lumped circuit. The size of the resonator should be smaller than a quarter of the resonant electromagnetic wavelength.

Flat-loop coil resonator

This resonator is composed of a parallel wire transmission line with a short-circuited loop at one end. RF electric and magnetic components distribute to the parallel line and the loop portion, respectively. In the original design, the resonator was mechanically matched to the RF line with a stub tuner[30]. Recent improvements have made the matching easy by the use of varactor diodes[31] or an electrical tuning circuit[32]. The latter is used with an automatic matching control (AMC), which is useful for reducing noise generated by animal movement. The sensitivity map for the flat-loop coil resonator is characteristic. Sensitivity is highest around the plane of the loop, and it decreases exponentially with increasing a distance between the plane and the sample. For this reason, this resonator has been used as a surface-coil-type resonator[33,34]. The imaging of cross sections is also possible if the sample is inserted into the loop[4,35].

Parallel coil resonator

Devasahayam *et al.*[36] designed a parallel coil resonator for 300 MHz ESR, which is equivalent to stacked flat-loop coils. It is used as a volume-coil-type resonator because sensitivity is homogeneous in the sample space.

APPLICATION OF *IN VIVO* ESR SPECTROSCOPY

Although the subjects of ESR spectroscopy are limited to compounds with an unpaired electron, the applications of *in vivo* ESR cover a broad range. Many investigators have applied *in vivo* ESR spectroscopy and its imaging to the physiological, medical, and pharmaceutical fields. pH in mouse stomach has been monitored with a pH-sensitive nitroxyl probe administered orally[37]. The metabolic fates of spin-labeled lipid particles[38], nitrosobenzene[39], and chromium[40] have also been studied in live mice. The most active use of *in vivo* ESR spectroscopy and its imaging has been in the measurements of redox status, radical generation, and partial pressure of oxygen.

Redox status

The pharmacokinetics of compounds carrying nitroxyl radical (nitroxyls) has been studied in animals and plants since the development of *in vivo* ESR spectrometers[10,14,27,41–44]. The kinetics of ESR signal decay of pyrrolidine nitroxyls (five-membered rings) and piperidine nitroxyls (six-membered rings) with various substituents was studied in mouse tail (3.5 GHz)[5], chest, and head (L-band)[8] after intravenous injection. The decay rates depended on both ring structures and the substituents of nitroxyls. The decay of pyrrolidine nitroxyls was generally slow compared with that of piperidine nitroxyls. The presence of charged groups in the substituents made the decay rate very low. The decay rates varied depending on the sites measured. Figure 4 shows the example of the difference in the signal decay between the head and upper abdomen of mice injected with a water-soluble nitroxyl radical, 3-carbamoyl-2,2,5,5-tetramethylpyrrolidine-*N*-oxyl (carbamoyl-PROXYL). The decay rate of the signal in the head was lower than in the upper abdomen. The difference in the decay rate depending on the sites was clearly demonstrated with a time course of a one-dimensional distribution of nitroxyl along the rat body axis[45]. The signal decay observed with the *in vivo* ESR measurement may result from the reduction, distribution and excretion of the nitroxyls. The signal reduction of water-soluble nitroxyls in blood was recovered almost completely by the addition of potassium hexacyanoferrate to the collected blood at 30 min after the intraperitoneal injection of the nitroxyls[9]. This suggests that the one-electron reduction of the nitroxyls to the corresponding hydroxylamines, which are ESR-silent forms, contributes largely to signal decay in the early stage. The decay was very slow in the collected blood[10], indicating that the reduction of nitroxyls occurs mainly in parenchymal cells. A one-electron reduction of nitroxyls also occurred in mouse lung[11,46]. A kinetic study revealed that sulfhydryl compounds act indirectly as electron donors in the reduction of nitroxyls in whole lung[47].

In vitro studies demonstrated that the reduction of nitroxyl radical was reversible in biological samples, such as liver

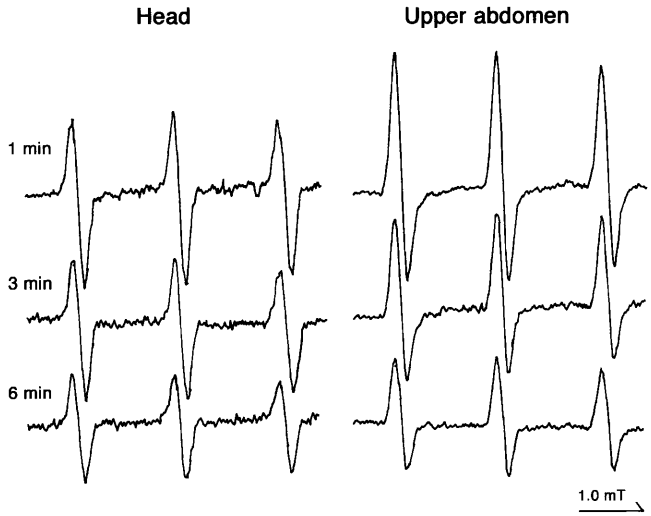

Fig. 4. ESR spectra of carbamoyl-PROXYL recorded in the head and upper abdomen of mice. An aqueous solution of carbamoy-PROXY (14 μmol) was intravenously injected to anesthetized mice. L-band ESR spectrum of carbamoyl-PROXYL was recorded in the head or upper abdomen with a JEOL RE 1X ESR spectrometer equipped with an L-band RF unit and a loop-gap resonator (33 mm i.d., 24 mm long). The amplitude of 100 kHz field modulation was 0.2 mT. Time after injection was indicated on the left hand side.

microsomes and cultured cells, depending on oxygen concentration[48–50]. Ascorbate and sulfhydryl compounds are involved in the reduction[51–53]. These observations indicate that nitroxyls are useful as redox probes (Scheme 1). An *in vivo* ESR study with an L-band ESR spectrometer equipped with a loop-gap resonator demonstrated that the *in vivo* decay rate of carbamoyl-PROXYL in the heads of old mice was lower than in young mice, whereas food restriction kept the decay rate in old mice at the level of young mice[9]. The decay rate of a water-soluble nitroxyl, 4-hydroxy-2,2,6,6-tetramethylpiperidine-*N*-oxyl, in rat heads was increased by giving antioxidants such as ascorbate, vitamin E, or idebenone along with food for 2 or 4 weeks, as measured with a 700 MHz ESR spectrometer with a loop-gap resonator[54,55]. The decay of carbamoyl-PROXYL, compared with controls, was significantly slower both in the upper abdomen and in the head of rats whose glutathione-peroxidase activity was suppressed by selenium deficiency, as measured with a 300 MHz ESR spectrometer[56].

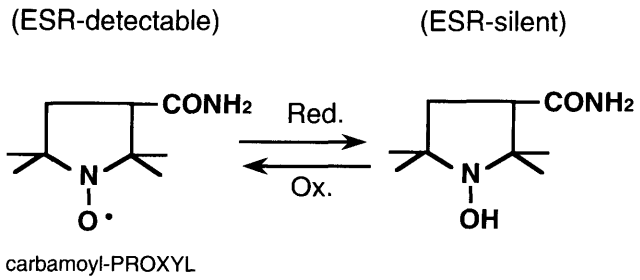

Scheme 1. Nitroxyl probe, carbamoyl-PROXYL, and its redox. Carbamoyl-PROXYL loses its ESR signal by a one-electron reduction. This reaction is reversible.

A lipid-soluble nitroxyl, 3-methoxycarbonyl-2,2,5,5-tetramethylpyrrolidine-*N*-oxyl (MC-PROXYL), distributes to the brain[57,58]. This was confirmed with 3-dimensional ESR imaging at L-band[59]. An ESR imaging technique at 700 MHz demonstrated that the half-life of MC-PROXYL was prolonged in the hippocampus of rats treated with kainic acid[60].

The decay rate of carbamoyl-PROXYL in radiation-induced fibrosarcoma (RIF-1) grown in mouse leg was compared with that in normal tissue using an L-band[61] and a 300 MHz ESR imaging system[62]. The decay rate of the nitroxyl in the tumor tissue was higher than normal and decreased by a depletion of glutathione[61,62]. Separately, a decline in the signal decay of carbamoyl-PROXYL was observed in the kidney and liver of Nrf2 transcription factor-deficient mice by the use of ESR imaging at L-band[63]. These studies demonstrate the usefulness of sequential images obtained after the probe injection for the analysis of site-specific rates of signal decay.

Radical reactions

Nitroxyl radical loses its paramagnetism not only by reduction, but also by reaction with ·OH and carbon-centered radicals at a nearly diffusion-controlled rate[64–66]. Signal reduction by peroxyl radicals was also reported[67]. Superoxide anion radical caused signal reduction in the presence of reductants such as sulfhydryl compounds and NAD(P)H ($k=10^{3-5}$ $M^{-1}s^{-1}$)[65,68,69]. As mentioned in the introduction, a direct detection of biological radicals with *in vivo* ESR spectroscopy is difficult. The reactivity of nitroxyls with some radicals suggests the feasibility of an indirect measurement of radical generation via the reduction of ESR signal of nitroxyls monitored by *in vivo* ESR spectroscopy. We examined the signal reduction of pyrrolidine and piperidine nitroxyls with various substituents by *in vitro* reaction with ·OH or $O_2^{\cdot-}$ plus reductants[65]. The signal reduction of piperidine nitroxyls varied depending on the substituents in both reaction systems, whereas that of pyrrolidine nitroxyls did not. Pyrroridine nitroxyls lost paramagnetism by reaction with ·OH at a near diffusion-controlled rate, but they were generally resistant to signal reduction by $O_2^{\cdot-}$ plus reductants. Furthermore, hydrogen peroxide and singlet oxygen caused no signal reduction in either pyrrolidine or piperidine nitroxyls. These observations suggest that pyrroridine nitroxyls are relatively specific to ·OH comparing with piperidine nitroxyls.

Miura *et al.* measured the rate of signal decay of carbamoyl-PROXYL intravenously injected in mice with an L-band ESR spectrometer equipped with a loop-gap resonator and observed an increase in the rate under hyperoxia[12]. They speculated that nitroxyl reacted with reactive oxygen species, resulting in a loss of paramagnetism, because the enhanced signal decay was suppressed by the preadministration of antioxidants such as glutathione, Trolox (a water-soluble analogue of vitamin E), and uric acid[70]. The irradiation of mice with X-rays (up to 15 Gy) also increased the decay rate of the carbamoyl-PROXYL signal 1 h after irradiation, and the increase was suppressed by the administration of cysteamine before the radiation[13]. The increase in the signal decay correlated with lipid peroxidation in the liver. The suppression effects on the increased signal decay caused by X-ray irradiation were screened with several radioprotective agents[71].

The subcutaneous administration of ferric citrate increased the decay rate of carbamoyl-PROXYL signal in mice[72]. This increase was suppressed by the administration of a chain-breaking antioxidant, Trolox. The administration of desferrioxamine, an iron-chelator, also suppressed the increased signal decay, depending on the time of administration with respect to iron loading. In that case there was a good correlation between the ESR signal decay and iron content and lipid peroxidation in the liver. Carbamoyl-PROXYL inhibited the lipid peroxidation of liver homogenates caused by iron citrate. These observations indicate the

relationship between the increase in the signal decay rate and the free radical reactions.

An increase in the decay rate of carbamoyl-PROXYL was also observed in rats with streptozotocin-induced diabetes by the use of a 300 MHz ESR spectrometer equipped with a loop-gap resonator[18]. It was suppressed by the administration of $O_2^{\cdot -}$ inhibitors, such as superoxide dismutase (SOD), 4,5-dihydroxy-1,3-benzene disulfonic acid (Tiron), allopurinol, and oxipurinol, indicating the increased generation of $O_2^{\cdot -}$ in the mice[73]. This was supported by an increased xanthin oxidase level in the plasma of the diabetic mice.

A membrane-impermeable nitroxyl probe may useful to measure radical generation in a localized area. Han *et al.*[74] injected a small volume of physiological solution of nitroxyl probe carrying a positively charged group, trimethylammonium-TEMPO, into mouse lung via the trachea and measured chest position with an L-band ESR spectrometer equipped with a loop-gap resonator. The ESR signal decreased with time at a rate much lower than that for carbamoyl-PROXYL injected intravenously. The reduction of nitroxyl should occur in the lung parenchymal cells[46,47]. The slow decay rate is probably due to the restricted diffusion of the probe into the cells for its charged group. The analyses of *in vivo* radical reactions with structurally different nitroxyl probes were recently reviewed[75].

The oxidation of hydroxylamine is an another potential index for radical reactions, because a hydroxylamine is easily oxidized by biological oxidants including reactive oxygen species to form nitroxyl radical. The apparent rate constants for the reaction of cyclic hydroxylamines with $O_2^{\cdot -}$ and peroxynitrite are 1.7×10^3–6.7×10^3 $M^{-1}s^{-1}$ and 4.5×10^9 $M^{-1}s^{-1}$, respectively[76,77]. A pioneer study performed in situ with hydroxylamine suggested the possibility of the detection of reactive oxygen species generated under oxidative stress such as the ischemia-reperfusion of organs[78]. Hydroxylamines are susceptible to auto-oxidation in an aqueous solution. Itoh *et al.*[79] introduced acyl-protected hydroxylamine probes to prevent auto-oxidation outside of biological systems. These probes were designed to be deprotected with esterase to yield corresponding hydroxylamines when they are injected into animals (Scheme 2). ESR imaging with 700 MHz ESR demonstrated that the signal intensity at the center part of the brain (probably hippocampus and striatum) after an injection of 1-acetoxy-3-carbamoyl-2,2,5,5-tetramethylpyrrolidine (ACP) was higher in rats with kainic acid-induced epileptic seizure than in control rats, suggesting the enhancement of oxidative stress in these parts after kainic acid treatment[80].

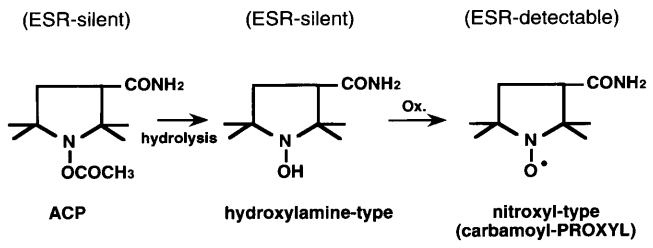

Scheme 2. Metabolism of acyl-protected hydroxylamine probe, ACP. ACP is readily hydrolyzed to hydroxylamine-type in *in vivo*. The hydroxylamine is oxidized to carbamoyl-PROXYL, having an ESR signal under oxidative condition.

We injected ACP into mice intravenously or intraperitoneally and examined its pharmacokinetics[81]. ACP injected intravenously was distributed quickly over most organs. A rapid hydrolysis of ACP occurred in the liver and kidney. The distribution of corresponding hydroxylamine was nearly homogeneous over most tissues 10 min after the injection of ACP regardless of the injection route. The level of hydroxylamine in the tissues was kept more than 30 min after the injection. These observations suggest that ACP is suitable to delineate the area where reactive oxygen species are produced in various disease models related to oxidative stress, using the *in vivo* ESR imaging technique.

Thus both nitroxyl radical and hydroxylamine are potential probes for the evaluation of radical reactions. However, it should be noted that the reactions of these probes are not specific to reactive oxygen species. The alterations of various reductase activities and antioxidant levels modify the redox state of these probes to affect the ESR signal intensity. Furthermore, if the pharmacokinetics of probes is changed in the disease model, it should also affect their signal intensity. Therefore the effects of administering appropriate radical scavengers on the disappearance or appearance of the ESR signal should be examined to assess the radical reactions by the use of the *in vivo* ESR technique with these probes.

Spin adducts of biological radicals

The direct detection of low concentrations of short-lived biological radicals is very difficult. A few research groups have reported the *in vivo* detection of spin adducts formed as a result of spin trapping biological radicals *in vivo*. The spin adducts of a conventionally used spin trap, 5,5-dimethyl-1-pyrroline-*N*-oxide (DMPO), are unstable in biological systems. Although the adducts of α-(4-pyridyl 1-oxide)-*N*-*tert*-butylnitrone (POBN) with carbon-centered radicals are stabler in biological systems, an adduct of this spin trap with ·OH is easily decomposed by itself. The ·OH reacts with ethanol and dimethyl sulfoxide at a near diffusion-controlled rate to generate 1-hydroxyethyl radical ($\cdot CH[OH]CH_3$) and methyl radical, respectively. These reactions appear specific to ·OH. Halpern *et al.*[82] injected POBN and ethanol into a tumor implanted in the leg of mouse, irradiated it with γ-rays at 3,000 Gy, and subjected it to 260 MHz ESR measurement. They observed the signal of the $\cdot CH[OH]CH_3$ adduct of POBN in the tumor. This was the first report about *in vivo* detection of reactive oxygen species by the use of *in vivo* ESR spectroscopy, though the radiation dose they used was

preposterous.

A recently developed spin trap, 5-diethoxyphosphoryl-5-methyl-1-pyrroline-*N*-oxide (DEPMPO), has some advantages in the stability of its spin adducts. Liu *et al.*[83] observed that the sulfur trioxide anion radical ($SO_3^{\cdot -}$) adduct of DEPMPO was much more stable than that of DMPO against reduction caused by ascorbic acid *in vitro*. They injected DEPMPO, sodium sulfite, and sodium dichromate into mice. The reaction of sulfite with dichromate produces $SO_3^{\cdot -}$[84]. They used this reaction as a model system for radical generation. When the mice set in a loop-gap resonator were measured with an L-band ESR spectrometer, a distinct signal for the $SO_3^{\cdot -}$ adduct of DEPMPO was recorded. Subsequently, an *in vivo* detection of the $^{\cdot}OH$ spin adduct was performed by the use of a similar method[85]. The $^{\cdot}OH$ generated by the reaction of $FeNH_4(SO_4)_2$ and 5-aminolevulinic acid in the mouse body was trapped with DEPMPO. An eight-line ESR spectrum whose hyperfine splitting constants were consistent with the $^{\cdot}OH$ adduct of DEPMPO was recorded, and a spectrum with hyperfine couplings characteristic of a carbon-centered radical adduct was recorded when dimethyl sulfoxide was injected into the mice. Thus they concluded that the $^{\cdot}OH$ adduct was, for the first time, detected *in vivo*. On the other hand, there is no report to date about *in vivo* detection of the $O_2^{\cdot -}$ adduct.

Nitric oxide ($NO^{\cdot}$) has also been subjected to *in vivo* ESR measurement. The reaction is summarized in Scheme 3. The formation of a paramagnetic mononitrosyl-iron complex as a result of trapping $NO^{\cdot}$ with diethyldithiocarbamate (DETC) *in vivo* was first reported by Vanin's group[86]. Lai *et al.*[6,7] developed water-soluble derivatives of dithiocarbamate, *N*-methyl-D-glucamine dithiocarbamate (MGD), and measured the ESR signal of the MGD_2-Fe^{2+}-NO complex in the tails of NO donor-injected mice and lipopolysaccharide (LPS)-induced septic-shock mice by the use of an S-band (3.5 GHz) ESR spectrometer equipped with a loop-gap resonator. The signal of the mononitrosyl-iron complex formed in LPS-treated mice was also detected in the abdominal region of DETC-injected mice by the use of an L-band ESR spectrometer equipped with a loop-gap resonator[87]. Yoshimura *et al.*[88] developed dithiocarbamate derivatives with more water solubility, *N*-(dithiocarboxy)sarcosine (DTCS). They injected a $DTCS_2$-Fe^{2+} complex into LPS-treated mice and observed the distinct three-line signal of the mononitrosyl iron complex in the abdominal region with a 700 MHz ESR spectrometer. Both ESR imaging and *in vitro* measurement of resected tissue indicated the presence of a high concentrations of the $DTCS_2$-Fe^{2+}-NO complex in the liver. Some dithiocarbamate derivatives of amino acids were synthesized, and their NO-trapping efficiency was examined in LPS-treated mice[89]. The mononitrosyl-iron complex was detected in the liver and blood for serine-derivatives, but the complex was detected only in the blood for proline-derivatives. When preformed MGD_2-Fe^{2+}-NO complex was intravenously injected into normal mice, a large fraction of the complex was recovered in the liver[90]. Therefore the pharmacokinetics of the dithiocarabamate-iron and mononitrosyl-iron complexes formed by NO-trapping contribute to the results observed with ESR spectroscopy. It should be especially noted that the observed distribution of the ESR signal does not always indicate the site of NO production.

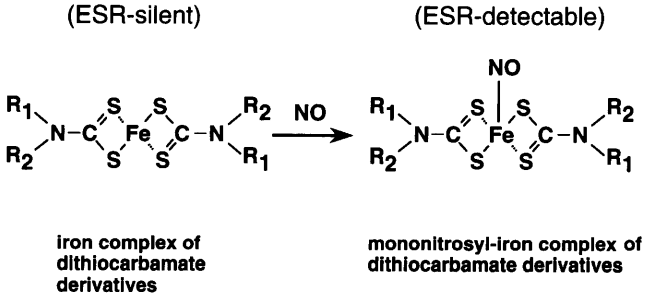

Scheme 3. Trapping of nitric oxide with dithiocarbamate-iron complexes. The water-solubility of dithiocarbamate-iron complexes is varied by using dithiocarbamate derivatives with different substituents (R_1 and R_2). The trapping of NO by dithiocarbamate-iron complexes results in the formation of ESR-detectable mononitrosyl-iron complexes.

Partial pressure of oxygen

Molecular oxygen in its ground state is biradical. Therefore the interaction of stable paramagnetic compounds with molecular oxygen shortens the ESR relaxation times of the compounds, resulting in an increase in the peak-to-peak line width of their ESR spectra. The increase in the line width correlates with a concentration of molecular oxygen. Thus this phenomenon can be used for the measurement of partial pressure of oxygen, pO_2 (ESR oximetry). Available paramagnetic probes fall into two types, water-insoluble particle type and water-soluble type. Lithium phtalocyanine[91], fusinite[92], synthetic chars[93], and India ink[94] are the former type, and nitroxyls[95–97] and triaryl methyl (trityl) radicals[98,99] are the latter. In some studies, nitroxyls were encapsulated into oxygen-permeable capillaries[95] and liposomes[96,100] to prevent the reduction and diffusion of the probes. Water-soluble probes were used for ESR imaging of the oxygen map, and water-insoluble probes and encapsulated nitroxyls were suitable for the topical measurement of pO_2.

Goda *et al.* implanted India ink in mouse mammary adenocarcinomas (MTG-B) and RIF-1 tumors in mouse legs and irradiated the tumors with X-rays[101]. As measured with an L-band ESR spectrometer, pO_2 levels in the MTG-B tumors were lower than those in RIF-1 tumors before irradiation. A temporal decrease in pO_2 was observed in both tumors after irradiation. The administration of insulin increased pO_2, measured with a charcoal probe, in transplantable liver tumors and syngeneic FSAII tumors in mouse legs, which correlated with the increase in the regrowth

delay caused by X-ray irradiation[102]. The effect of a chemotherapeutic drug, vinblastine, on pO_2 was also examined in another tumor model[103]. In RIF-1 tumors, pO_2, measured with lithium phthalocyanine, increased by carbogen-breathing[104].

Velan *et al*[97] obtained pO_2 images of mouse tails by the use of a spectral-spatial technique that makes it possible to separate spectral and spatial information. Spectral-spatial imaging with CW-ESR spectroscopy requires a very high field gradient, and consequently the diameter of the sample is limited.

Recent progress in electrical technology has enabled pulsed-radiofrequency ESR imaging of stable radicals with short relaxation times[105,106]. The interaction of the radical with molecular oxygen shortens the overall time of free induction decay of the excited radical with a short RF pulse. With the use of this time difference, which depends on oxygen concentration, a trial study was performed by Subramanian *et al.*[107] to obtain ESR images of oxygen maps of *scc* tumors in mouse leg without a large field gradient.

CONCLUSION

Although the direct measurement of biological radicals is presently difficult, several studies have been performed with *in vivo* ESR spectroscopy. This may indicate the necessity of the *in vivo* evaluation of radical generation and redox status. The knowledge of the generation routes of radicals is important to clarify mechanisms related to diseases and injuries caused by radiation, ischemia-reperfusion, and other oxidative factors. The pO_2 level should closely relate to the generation of radicals and the progression of their reactions. The sensitivity of the *in vivo* ESR instruments and the specificity and stability of probes are, at present, insufficient. Further improvements of the instruments and probes may give us much more information about the mechanisms for the diseases and injuries from the viewpoints of radical generation and redox status.

ACKNOWLEDGMENTS

This work was supported in part by the Life Science Foundation of Japan and the AOB Japan Research Foundation. We thank Dr. J. J. Rodrigue for editing the manuscript.

REFERENCES

1. Buettner, G. R. (1987) Spin trapping: ESR parameters of spin adducts. Free Radic. Biol. Med. **3**: 259–303.
2. Halpern, H. J. and Bowman, M. K. (1991) Low-frequency EPR spectrometers: MHz range. In "EPR imaging and *in vivo* EPR" Eds. Eaton, G.R., Eaton, S.S. and Ohno, K. pp.45–63, CRC press, Inc., Boca Raton.
3. Lukiewicz, S. J., Lukiewicz, S. G. (1984) *In vivo* ESR spectroscopy of large biological objects. Magn. Reson. Med. **1**:297–298.
4. Berliner, L. J., Fujii, H., Wan, X. M. and Lukiewicz, S. J. (1987) Feasibility study of imaging a living murine tumor by electron paramagnetic resonance. Magn. Reson. Med. **4**: 380–384.
5. Komarov, A. M., Joseph, J. and Lai, C.-S. (1994) *In vivo* pharmacokinetics of nitroxides in mice. Biochem. Biophys. Res. Commun. **201**: 1035–1042.
6. Komarov, A., Mattson, D., Jones, M. M., Singh, P. K. and Lai, C.-S. (1993) *In vivo* spin trapping of nitric oxide in mice. Biochem. Biophys. Res. Commun. **195**: 1191–1198.
7. Lai, C.-S. and Komarov, A. M. (1994) Spin trapping of nitric oxide produced *in vivo* in septic-shock mice. FEBS Lett. **345**: 120–124.
8. Utsumi, H. and Takeshita, K. (1995) *In vivo* ESR measurement of free radical reactions in living animals using nitroxyl probes. In: "Bioradicals detected by ESR Spectroscopy" Eds. Ohya-Nishiguchi, H. and Packer, L. pp.321–334, Birkhauser Verlag base, Switzerland.
9. Gomi, F., Utsumi, H., Hamada, A. and Matsuo, M. (1993) Aging retards spin clearance from mouse brain and food restriction prevents its age-dependent retardation. Life Sciences. **52**: 2027–2033.
10. Utsumi, H., Muto, E., Masuda, S. and Hamada, A. (1990) *In vivo* ESR measurement of free radicals in whole mice. Biochem. Biophys, Res. Commun. **172**: 1342–1348.
11. Takeshita, K., Utsumi, H. and Hamada, A. (1991) ESR measurement of radical clearance in lung of whole mouse. Biochem. Biophys. Res. Commun. **177**: 874–880.
12. Miura, Y., Utsumi, H. and Hamada, A. (1992) Effects of inspired oxygen concentration on *in vivo* redox reaction of nitroxide radicals in whole mice. Biochem. Biophys. Res. Commun. **182**: 1108–1114.
13. Miura, Y., Anzai, K., Urano, S. and Ozawa, T. (1997) electron paramagnetic resonance studies on oxidative stress caused by x-irradiation in whole mice. Free Radic. Biol. Med. **23**: 533–540.
14. Ferrari, M., Colacicchi, S., Gualtieri, G., Santini, M.T. and Sotgiu, A. (1990) Whole mouse nitroxide free radical pharmacokinetics by low frequency electron paramagnetic resonance. Biochem. Biophys. Res. Commun. **166**: 168–173.
15. Quaresima, V., Alecci, M., Ferrari, M. and Sotgiu, A. (1992) Whole rat electron paramagnetic resonance imaging of a nitroxide free radical by a radio frequency (280 MHz) spectrometer. Biochem. Biophys. Res. Commun. **183**: 829–835.
16. Ishida, S., Matsumoto, S., Yokoyama, H., Mori, N., Kumashiro, H., Tsuchihashi, N., Ogata, T., Yamada, M., Ono, M., Kitajima, T., Kamada, H. and Yoshida, E. (1992) An ESR-CT imaging of the rat head of a living rat receiving an administration of a nitroxide radical. Magn. Reson. Imaging **10**: 109–114.
17. Yokoyama, H., Itoh, O., Ogata, T., Obara, H., Ohya-Nishiguchi, H. and Kamada, H. (1997) Temporal brain imaging by a rapid scan ESR–CT system in rats receiving intraperitoneal injection of a methyl ester nitroxide radical. Magn. Reson. Imaging **15**: 1079–1084.
18. Sano, T., Umeda, F., Hashimoto, T., Nawata, H. and Utsumi,

H. (1998) Oxidative stress measurement by *in vivo* electron spin resonance spectroscopy in rats with streptozotocin-induced diabetes. Diabetology **41**: 1355–1360.
19. Ohno, K. (1986) ESR imaging and its applications. Appl. Spec. Rev. **22**: 1–56.
20. Eaton, G. R., Eaton, S. S. and Ohno, K. (1991) EPR imagingand *in vivo* EPR, CRC Press, Inc., BocaRaton, FL.
21. Berliner, L. J., Fujii, H., (1985) Magnetic resonance imaging of biological specimens by electron paramagnetic resonance of nitroxide spin labels. Science **227**: 517–519.
22. Poole, C. P. Jr. (1983) Electron spin resonance: A comprehensive treatise on experimental techniques, second edition, pp.381–458, John Willy & Sons, New York.
23. Froncisz, W. and Hyde, J. S.(1982) The loop-gap resonator: A new microwave lumped circuit ESR sample structure. J. Magn. Reson. **47**: 515–521.
24. Ono, M., Ogata, T., Hsieh, K. C., Suzuki, M., Yoshida, E. and Kamada, H. (1986) L-band ESR spectrometer using a loop-gap resonator for *in vivo* analysis. Chem. Lett. 491–494.
25. Ono, M., Suenaga, A. and Hirata, H. (2002) Experimental investigation of RF magnetic field homogeneity in a bridged loop-gap resonator. Magn. Reson. Med. **47**: 415–419.
26. Zweier, J. L. and Kuppusamy, P. (1988) Electron paramagnetic resonance measurements of free radicals in the intact beating heart: a technique for detection and characterization of free radicals in whole biological tissues. Proc. Natl. Acad. Sci. USA **85**: 5703–5707.
27. Kuppusamy, P., Wang, P., Shankar, R. A., Ma, L., Trimble, C. E., Hsia, C. J. C. and Zweier, J. L. (1998) *In vivo* topical EPR spectroscopy and imaging of nitroxide free radicals and polynitroxyl-albumin. Magn. Reson. Med. **40**: 806–811.
28. Sotgiu, A. (1985) Resonator design for *in vivo* ESR spectroscopy. J. Magn. Reson. **65**: 206–214.
29. Giordano, M., Momo, F. and Sotgiu, A. (1983) On the design of re-entrant square cavity. J. Phys. E: Sci. Instrum. **16**: 774–779.
30. Nishikawa, H., Fujii, H. and Berliner, L. J. (1985) Helices and surface coils for low-field *in vivo* ESR and EPR imaging applications, J. Magn. Reson. **62**: 79–86.
31. Hirata, H. and Ono, M. (1997) Impedance-matching system for a flexible surface-coil-type resonator. Rev. Sci. Instrum. **68**: 3528–3532.
32. Hirata, H. Walczak, T. and Swartz, H.M. (2000) Electrically tunable surface-coil-type resonator for L-band EPR spectroscopy. J. Magn. Reson. **142**: 159–167.
33. Lin, Y., Yokoyama, H., Ishida, S., Tsuchihashi, N. and Ogata, T. (1997) *In vivo* electron spin resonance analysis of nitroxide radicals injected into a rat by a flexible surface-coil-type resonator as an endoscope- or a stethoscope-like device. MAGMA **5**: 99–103.
34. Takeshita, K., Takajo, T., Hirata, H., Ono, M. and Utsumi, H. (2004) *In vivo* oxygen radical generation in the skin of the protoporphyria model mouse with visible light exposure: an L-band ESR study. J. Invest. Dermatol. **122**: 1463–1470.
35. Ueda, A., Yokoyama, H., Nagase, S., Hirayama, A., Koyama, A., Ohya, H. and Kamada, H. (2002) *In vivo* temporal EPR imaging for estimating the kinetics of a nitroxide radical in the renal parenchyma and pelvis in rats. Magn. Reson. Imaging **20**: 77–82.
36. Devasahayam, N., Subramanian, S., Murugesan, R., Cook, J. A., Afeworki, M., Tschudin, R. G., Mitchell, J. B. and Krishna, M. C. (2000) Parallel coil resonators for time-domain radiofrequency electron paramagnetic resonance imaging of biological objects. J. Magn. Reson. **142**: 168–176.
37. Gallez, B., Mader, K. and Swartz, H.M. (1996) Noninvasive measurement of the pH inside the gut by using pH-sensitive nitroxides. An *in vivo* EPR study. Magn. Reson. Med. **36**: 694–697.
38. Yamaguchi, T., Itai, S., Hayashi, H., Soda, S., Hamada, A. and Utsumi, H. (1996) *In vivo* ESR studies on pharmacokinetics and metabolism of parenteral lipid emulsion in living mice. Pharmaceu. Res. **13**: 729–733.
39. Fujii, H., Zhao, B., Koscielniak, J. and Berliner L.J. (1994) *In vivo* EPR studies of the metabolic fate of nitrosobenzene in the mouse. Magn. Reson. Med. **31**: 77–80.
40. Liu, K. J., Jiang, J. J., Swartz, H. M. and Shi, X. (1994) Low-frequency EPR detection of chromium (V) formation from chromium (VI) in whole mice. Ach. Biochem. Biophys. **313**: 248–252.
41. Berliner, L. J. and Wan, X. (1989) *In vivo* pharmacokinetics by electron magnetic resonance spectroscopy. Magn. Reson. Med. **9**: 430–434.
42. Bacic, G., Nilges, M. J., Magin, R. L., Walczak, T. and Swartz, H. M. (1989) *In vivo* localized ESR spectroscopy reflecting metabolism. Magn. Reson. Med. **10**: 266–272.
43. Ogata, T., Ono, M., Fujisawa, T., Yoshida, E. and Kamada, H. (1986) An example of *in vivo* analysis by L-band ESR technique using a loop-gap resonator. Chem. Lett. 1681–1684.
44. Masuda, S., Utsumi, H. and Hamada, A. (1991) *In vivo* ESR study on diffusion of spin labeled compounds in femoral muscle. Magn. Reson. Med. Jpn. **2**: 69–74.
45. Alecci, M., Ferrari, M., Quaresima, V., Sotgiu, A. and Ursini, C. L. (1994) Simultaneous 280 MHz EPR imaging of rat organs during nitroxide free radical clearance. Biophys. J. **67**: 1274–1279.
46. Takeshita, K., Utsumi, H. and Hamada, A. (1993) Whole mouse measurement of paramagnetism-loss of nitroxide free radical in lung with a L-band ESR spectrometer. Biochem. Mol. Biol. Int. **29**: 17–24.
47. Takeshita, K., Hamada, A. and Utsumi, H. (1999) Mechanisms related to reduction of radical in mouse lung using an L-band ESR spectrometer. Free Radic. Biol. Med. **26**: 951–960.
48. Rosen, G. M. and Rauckman, E. J. (1977) Formation and reduction of a nitroxide radical by liver microsomes. Biochem. Pharmacol. **26**: 675–678.
49. Chen, K. and swartz, H. M. (1988) Oxidation of hydroxylamines to nitroxide spin labels in living cells. Biochim. Biophys. Acta **970**: 270–277.
50. Chen, K.. Glockner, J. F., Morse II, P. D. and Swartz, H. M. (1989) Effects of oxygen on the metabolism of nitroxide spin labels in cells. Biochemistry **28**: 2496–2501.
51. Couet, W. R., Brasch, R. C., Sosnovsky, G. and Tozer, T. N.

(1985) Factors affecting nitroxide reduction in ascorbate solution and tissue homogenates. Magn. Reson. Imaging **3**: 83–88.
52. Eriksson, U. G., Brasch, R. C. and Tozer, T. (1987) Nonenzymatic bioreduction in rat liver and kidney of nitroxyl spin labels, potential contrast agents in magnetic resonance imaging. Drug Metabol. Dispos. **15**: 155–160.
53. Iannone, A., Tomasi, A., Vannini, V. and Swartz, H. M. (1990) Metabolism of nitroxide spin labels in subcellular fractions of rat liver. II. Reduction in the cytosol. Biochim. Biophys. Acta **1034**: 290–293.
54. Yokoyama, H., Tuchihashi, N., Hiramatsu, M. and Mori, A. (1996) An analysis of the intracerebral ability to eliminate a nitroxide radical in the rat after administration of idebenone by an *in vivo* rapid scan electron spin resonance spectrometer. MAGMA **4**: 247–250.
55. Matsumoto, S., Mori, N., Tsuchihashi, N., Ogata, T., Lin, Y., Yokoyama, H. and Ishida, S. (1998) Enhancement of nitroxide-reducing activity in rats after chronic administration of vitamin E, vitamin C, and idebenone examined by an *in vivo* electron spin resonance technique. Magn. Reson. Med. **40**: 330–333.
56. Matsumoto, K., Endo, K. and Utsumi, H. (2000) *In vivo* electron spin resonance assessment of decay constant of nitroxyl radical in selenium-deficient rat. Biol. Pharmaceu. Bull. **23**: 641–644.
57. Sano, H., Matsumoto, K. and Utsumi, H. (1997) Synthesis and imaging of blood-brain-barrier permeable nitroxylorobes for free radical reactions in brain of living mice. Biochem. Mol. Biol. Int. **42**: 641–647.
58. Miura, Y., Anzai, K., Takahashi, S. and Ozawa, T. (1997) A novel lipophilic spin probe for the measurement of radiation damage in mouse brain using *in vivo* electron spin resonance (ESR). FEBS Lett. **419**: 99–102.
59. Anzai, K., Saito, K., Takeshita, K., Takahashi, S., Miyazaki, H., Shoji, H., Lee, M.-C., Masumizu, T. and Ozawa, T. (2003) Assessment of ESR-CT imaging by comparison with autoradiography for the distribution of a blood-brain-barrier permeable spin probe, MC-PROXYL, to rodent brain. Magn. Reson. Imaging **21**: 765–772.
60. Yokoyama, H., Lin, Y., Itoh, O., Ueda, Y., Nakajima, A., Ogata, T., Sato, T., Ohya-Nishiguchi, H. and Kamada, H. (1999) EPR imaging for *in vivo* analysis of the half-life of a nitroxide radical in the hipocampus and cerebral cortex of rats after epileptic seizures. Free Radic. Biol. Med. **27**: 442–448.
61. Kuppusamy, P., Li, H., Ilangovan, G., Cardounel, A.J., Zweier, J.L., Yamada, K., Krishna, M.C. and Mitchell, J.B. (2002) Noninvasive imaging of tumor redox status and its modification by tissue glutathione level. Cancer Res. **62**: 307–312.
62. Yamada, K., Kuppusamy, P., Yoo, J., Irie, A., Subramanian, S., Mitchell, J.B. and Krishna, M. C. (2002) Feasibility and assessment of non-invasive *in vivo* redox status using electron paramagnetic resonance imaging. Acta Radiol. **43**: 433–440.
63. Hirayama, A., Yoh, K., Nagase, S., Ueda, A., Itoh, K., Morito, N., Hirayama, K., Takahashi, S., Yamamoto, M. and Koyama, A. (2003) EPR imaging of reducing activity in Nrf2 transcriptional factor-deficient mice. Free Radic. Biol. Med. **34**: 1236–1242.
64. Fuchs, J., Groth, N., Herrling, T. and Zimmer, G. (1997) Electron paramagnetic resonance studies on nitroxide radical 2255-tetramethyl-4-piperidin-1-oxyl (TEMPOL) redox reactions in human skin. Free Rad. Biol. Med. **22**: 967–976.
65. Takeshita, K., Saito, K., Ueda, J., Anzai, K. and Ozawa, T. (2002) Kinetic study on ESR signal decay of nitroxyl radicals, potent redox probes for *in vivo* ESR spectroscopy, caused by reactive oxygen species. Biochim. Biophys. Acta, **1573**: 156–164.
66. Chateauneuf, J., Lusztyk, J. and Ingold, K.U. (1988) Absolute rate constants for the reactions of some carbon-centered radicals with 2266-tetramethylpiperidine-N-oxyl. J. Org. Chem. **53**: 1629–1632.
67. Takahashi, M., Tsuchiya, J. and Niki, E. (1989) Scavenging of radicals by vitamin E in the membranes as studied by spin labeling. J. Am. Chem. Soc. **111**: 6350–6353.
68. Finkelstein, E., Rosen., G. M. and Rauckman, E. J. (1984) Superoxide-dependent reduction of nitroxides by thiols. Biochim. Biophys. Acta **802**: 90–98.
69. Krishna, M. C., Grahame, D. A., Samuni, A., Mitchell, J. B. and Russo, A. (1992) Oxoammonium cation intermediate in the nitroxide-catalyzed dismutation of superoxide. Proc. Natl. Acad. Sci. USA **89**: 5537–5541.
70. Miura, U., Hamada, A. and Utsumi, H. (1995) *In vivo* ESR studies of antioxidant activity on free radical reaction in living mice under oxidative stress. Free Radic. Res. **22**: 209–214.
71. Miura, Y., Anzai, K., Ueda, J. and Ozawa, T. (2000) Novel approach to *in vivo* screening for radioprotective activity in whole mice: *in vivo* electron spin resonance study probing the redox reaction of nitroxyl. J. Radiat. Res. **41**: 103–111.
72. Phumala, N., Ide, T. and Utsumi, H. (1999) Non invasive evaluation of *in vivo* free radical reactions catalyzed by iron using *in vivo* ESR spectroscopy. Free Radic. Biol. Med. **26**: 1209–1217.
73. Matsumoto, S., Koshiishi, I., Inoguchi, T., Nawata, H. and Utsumi H. (2003) Confirmation of superoxide generation via xanthine oxidase in streptozotocin-induced diabetic mice. Free Radic. Res. **37**: 767–772.
74. Han, J.-Y., Takeshita, K. and Utsumi, H. (2001) Noninvasive detection of hydroxyl radical generation in lung by diesel exhaust particles. Free Radic. Biol. Med. **30**: 516–525.
75. Utsumi, H., Yamada, K. (2003) *In vivo* electron spin resonance-computed tomography/nitroxyl probe technique for non-invasive analysis of oxidative injuries. Arch. Biochem. Biophys. **416**: 1–8.
76. Rosen, G. M., Finkelstein, E. and Rauckman, E. J. (1982) A method for the detection of superoxide in biological systems. Arch. Biochem. Biophys. **215**: 367–378.
77. Dikalov, S., Skatchkov, M. and Bassenge, E. (1997) Spin trapping of superoxide radicals and peroxynitrite by 1-hydroxy-3-carboxy-pyrrolidine and 1-hydroxy-2,2,6,6-tetramethyl-4-oxo-piperidine and the stability of corresponding nitroxyl radicals towards biological reductants. Biochem. Biophys. Res. Commun. **231**: 701–704.

78. Nilsson, U. A., Lundgren, O., Haglind, E. and Bylund-Fellenius, A.-C. (1989) Radical production during *in vivo* intestinal ischemia and reperfusion in the cat. Am. J. Physiol. **257**: G409–414.
79. Itoh, O., Aoyama, M., Yokoyama, H., Obara, H., Ohya, H. and Kamada, H. (2000) Sensitive ESR deetermination of intracellular oxidative stress by using acyl-protected hydroxylamines as new spin reagents. Chem. Lett. 304–305.
80. Yokoyama, H., Itoh, O., Aoyama, M., Obara, H., Ohya, H. and Kamada, H. (2000) *In vivo* EPR imaging by using an acyl-protected hydroxylamine to analyze intracerebral oxidative stress in rats after epileptic seizures. Magn. Reson. Imaging. **18**: 875–879.
81. Saito, K., Takeshita, K. Anzai, K. and Ozawa, T. (2004) Pharmacokinetic study of acyl-protected hydroxylamine probe, 1-acetoxy-3-carbamoyl-2,2,5,5-tetramethylpyrrolidine, for *in vivo* measurements of reactive oxygen species. Free Radic. Biol. Med. **36**: 517–525.
82. Halpern, H. J., Yu, C., Barth, E., Peric, M. and Rosen, G.M. (1995) In situ detection, by spin trapping, of hydroxyl radical markers produced from ionizing radiation in the tumor of a living mouse. Proc. Natl. Acad. Sci. USA **92**: 796–800.
83. Liu, K. J., Miyake, M., Panz, T. and Swartz, H. (1999) Evaluation of DEPMPO as a spin trapping agent in biological systems. Free Radic. Biol. Med. **26**: 714–721.
84. Ozawa, T., Kwan, T. (1985) ESR studies on the preparation of the sulphite radical anion, SO_3^-, in aqueous solution. Polyhedron **4**: 1995–1996.
85. Timmins, G. S., Liu, K. J., Bechara, J. H., Kotake, Y. and Swartz, H. M. (1999) Trapping of free radicals with direct *in vivo* EPR detection: A comparison of 5,5-dimethyl-1-pyrroline-N-oxide and 5-diethoxyphosphoryl-5-methyl-1-pyrroline-*N*-oxide as spin traps for HO. and $SO_4^{\cdot-}$. Free Radic. Biol. Med. **27**: 329–333.
86. Kubrina, L. N., Caldwell, W. S., Mordvintcev, P. I., Malenkova, I.V. and Vanin, A.F. (1992) EPR evidence for nitric oxide production from guanidino nitrogens of L-arginine in animal tissues *in vivo*. Biochim Biophys. Acta **1099**: 233–237.
87. Quaresima, V., Takehara, H., Tsushima, K., Ferrari, M. and Utsumi, H. (1996) *In vivo* detection of mouse liver nitric oxide generation by spin trapping electron paramagnetic resonance spectroscopy. Biochem. Biophys. Res. Commun.. **221**: 729–34.
88. Yoshimura, T., Yokoyama, H., Fujii, S., Takayama, F., Oikawa, K. and Kamada, H. (1996) *In vivo* EPR detection and imaging of endogenous nitric oxide in lipopolysaccharide-treated mice. Nature Biotechnology **14**: 992–994.
89. Nakagawa, H., Ikota, N., Ozawa, Masumizu, T. and Kohno, M. (1998) Soin trapping for nitric oxide produced in LPS-treated mouse using various new dithiocarbamate iron complexes having substituted proline and serine moiety. Biochem. Mol. Biol. Int. **45**: 1129–1138.
90. Takeshita, K., Tsushima, K., Takehara, H. and Utsumi, H. (1997) Whether does *in vivo* NO-trapping with dithiocarbamate-iron complex give information about generation site of NO? -Approach from pharmacokinetics of nitrosyl dithiocarbamate-iron complex. Abstracts for 2nd International Conference on Bioradicals ans 5th International Workshop on ESR(EPR) Imaging and *in vivo* ESR Spectroscopy. pp. 43.
91. Liu, K. J., Gast, P., Moussavi, M., Norby, S. W., Vahidi, N., Walczak, T., Wu, M. and Swartz, H. M. (1993) Lithium phthalocyanine: a probe for electron paramagnetic resonance oximetry in viable biological systems. Proc. Natl. Acad. Sci. USA **90**: 5438–5442.
92. Vahidi, N., Clarkson, R. B., Liu, K.J., Norby, S. W., Wu, M. and Swartz, H. M. (1994) *In vivo* and in vitro EPR oximetry with fusinite: a new coal-derived, particulate EPR probe. Magn. Reson. Med. **31**: 139–146.
93. Zweier, J. L., Chzhan, M., Ewert, U., Schneider, G. and Kuppusamy, P. (1994) Development of a highly sensitive probe for measuring oxygen in biological tissues. J. Magn. Reson. B **105**: 52–57.
94. Swartz, H. M., Liu, K. J., Goda, F. and Walczak, T. (1994) India ink: a potential clinically applicable EPR oximetry probe. Magn. Reson. Med. **31**: 229–232.
95. Subczynski, W. K., Lukiewicz, S. and Hyde, J. S. (1986) Murine *in vivo* L-band ESR spin-label oximetry with a loop-gap resonator. Magn. Reson. Med. **3**: 747–754.
96. Chan, H.-C,, Glockner, J. F. and Swartz, H. M. (1989) Oximetry in cells and tissues using a nitroxide-liposome system. Biochim. Biophys. Acta **1014**: 141–144.
97. Valan, S. S., Spencer, R. G. S., Zweier, J. L. and Kuppusamy, P. (2000) Electron paramagnetic resonance oxigen mapping (EPROM): direct visualization of oxygen concentration in tissue. Magn. Reson. Med. **43**: 804–809.
98. Ardenkjaer-Larsen, J. H., Laursen, I., Leunbach, I., Ehnholm, G., Wistrand, L. G., Petersson, J. S. and Golman, K. (1998) EPR and DNP properties of certain novel single electron contrast agents intended for oximetric imaging. J. Magn. Reson. **133**: 1–12.
99. Subramanian, S., Yamada, K., Irie, A., Murugesan, R., Cook, J. A., Devasahayam, N., Van Dam, G. M., Mitchell, J. B. and Krishna, M. C. (2002) Noninvasive *in vivo* oxymetric imaging by radiofrequency FT EPR. Magn. Reson. Med. **47**: 1001–1008.
100. Glockner, J. F., Chan, H.-C. and Swartz, H. M. (1991) *In vivo* oximetry using a nitroxide-liposome system. Magn. Reson. Med. **20**: 123–133.
101. Goda, F., O'Hara, J.A., Rhodes, E. S., Liu, K. J., Dunn, J. F., Bacic, G. and Swartz, H. M. (1995) Changes of oxygen tension in experimental tumors after a single dose of X-ray irradiation. Cancer Res. **55**: 2249–2252.
102. Jordan, B. F., Gregoire, V., Demeure, R. J., Sonveaux, P., Feron, O., O'Hara, J., Vanhulle, V. P., Delzenne, N. and Gallez, B. (2002) Insulin increases the sensitivity of tumores to irradiation: involvement of an increase in tumore oxigenation mediated by a nitric oxide-dependent decrease of the tumor cells oxygen consumption. Cancer. Res. **62**: 3555–3561.
103. Sersa, G., Krzic, M., Sentjurc, M., Ivanusa, T., Beravs, K., Cemazar, M., Auersperg, M. and Swartz, H.M. (2001) Reduced tumor oxygenation by treatment with vinblastine. Cancer Res. **61**: 4266–4271.
104. Ilangovan, G., Li, H., Zweier, J. L., Krishna, M. C., Mitchell,

J. B. and Kuppusamy, P. (2002) *In vivo* measurement of regional oxygenation and imaging of redox states in RIF-1 murine tumor: effect of carbogen-breathing. Magn. Reson. Med. **48**: 723–730.

105. Murugesan, R., Cook, J. A., Devasahayam, N., Afeworki, M., Subramanian, S., Tschudin, R., Larsen, J. A., Mitchell, J. B., Russo, A. and Krishna, M. C. (1997) *In vivo* imaging of a stable paramagnetic probe by pulsed-radiofrequency electron paramagnetic resonance spectroscopy. Magn. Reson. Med. **38**: 409–414.
106. Afeworki, M., Van Dam, G. M., Devasahayam, N., Murugesan, R., Cook, J. A., Coffin, D., A.-Larsen, J. H., Mitchell, J. B., Subramanian, S. and Krishna, M. C. (2000) Three-dimentional whole body imaging of spin probes in mice by time-domain radiofrequency electron paramagnetic resonance. Magn. Reson. Med. **43**: 375–382.
107. Subramanian, S., Yamada, K., Irie, A., Murugesan, R., Cook, J., Devasahayam, N., Van Dam, G. M., Mitchell, J. B. and Krishna, M.C. (2002) Noninvasive *in vivo* oximetric imaging by radiofrequency FT EPR. Magn. Reson. Med. **47**: 1001–1008.

Received on March 2, 2004
1st Revision on July 5, 2004
Accepted on July 14, 2004